Assisting Physical (Hydro)Therapy With Wireless Sensors Networks

Renan C. A. Alves, Lucas Batista Gabriel, Bruno Trevizan de Oliveira,
Cíntia Borges Margi, *Member, IEEE*, and Fabíola Carvalho Lopes dos Santos

***Abstract*—Wireless sensor networks (WSNs) and Internet of Things (IoT) have been used to build several eHealth systems, which enable a physician (or caregiver) to monitor a patient (or elderly) continuously and real time, either locally or remotely, at lower cost and being less intrusive in the routine than the traditional monitoring equipment. Physical therapy aiding systems are a particular case of such systems, with specific characteristics and requirements, concerning equipment, software, and system. This work presents a system aimed at assessing joint angle and vital signs to assist physical therapists. The system is also available to hydrotherapy, which imposes packaging, sensing, and communication challenges. We discuss our design and implementation, as well as common problems with this kind of application. We also present statistical analysis of the system results based on experiments conducted and compared to a goniometer, a standard physical therapy device.**

***Index Terms*—Physical therapy, underwater communication, wireless sensor networks (WSN).**

I. Introduction

INTERNET of Things (IoT) is the network of physical objects accessed through the Internet [1]. These objects can sense, process, and communicate, and thus increase the information and perception about the world. Wireless sensor networks (WSNs) are an important component of IoT, which could be applied to improve WSN-based eHealth systems [2], [3], since such systems enable continuous real-time, local, or remote, monitoring a patient or elderly for a physician or a caregiver, at lower cost and being less intrusive in the routine. Almendar and Ersoy [3] surveyed WSN for health-care organizing them into five groups: 1) activity of daily living monitoring; 2) fall and movement detection; 3) location tracking; 4) medication intake monitoring; and 5) medical status monitoring.

As pointed out by Hadjidj *et al.* [4], rehabilitation supervision has different intrinsic requirements than general health-care monitoring systems, such as sensor nodes' unobtrusiveness, sensor fixation, energy efficiency, body impact on signal propagation, reliability, quality of service (QoS), routing, calibration, synchronization, and feedback. The same requirements apply to assisting physical therapy in a clinic.

For instance, sensor nodes' unobtrusiveness could be achieved with really small sensor nodes, whose size is usually limited by the battery size, which in turn limits the amount of energy available and how long the system could run without charging or replacing batteries. When used to assist physical therapy, multiple sensor nodes should be fixed in very specific positions of the body. If sensors move during a session, or if they are not in the correct position, data obtained will not be accurate and could lead to wrong motion information concerning the movement or activity being performed by the patient. Concerning communication, each sensor type has specific necessary data acquisition rates and thus requires specific bandwidth to be sent to the processing/monitoring station. Also, the network should provide reliability and QoS through MAC and routing protocols.

For WSN systems, besides these specific requirements concerning assisting physical therapy, one should also consider what devices are typically available in clinics. Considering range of motion, an important parameter used for evaluation and physical therapy treatment, the most widely used device to measure joint angles is the goniometer [5]. To measure a joint angle using the goniometer, the therapist must stop the patient's activity, place the device, and then read the corresponding angle. If the therapist needs to monitor heart rate or pressure during a rehabilitation session, he/she must stop the patient's activity and measure/monitor these health parameters.

Our work focuses on assisting a physical therapist through the rehabilitation process, both on soil and in water (hydrotherapy). Given these unique characteristics of a WSN-based physical therapy systems, our contribution is to design, develop, deploy, and validate such system. The designed WSN-based system provides real-time supervision, assessing joint angles and medical data, such as oxygen saturation and pulse.

We also consider as requirements the use of off-the-shelf hardware, standard communication protocols (such as the IEEE802.15.4 MAC layer), and that the software interface be easy to configure and to use to obtain feedback. The use of off-the-shelf hardware would allow for lower cost, medical and communication agencies approval, and readily available technical assistance. Also, off-the-shelf hardware should be standard compatible, and thus a good choice is the IEEE 802.15.4 standard, which has a time-slotted operation mode that could be used to ensure reliable delivery and QoS. The software interface must provide good feedback to both the physical therapist and

Manuscript received May 30, 2014; revised December 23, 2014; accepted January 09, 2015. Date of publication January 22, 2015; date of current version March 13, 2015. This work was supported by Microsoft Research.

R. C. A. Alves, L. Batista Gabriel, B. Trevizan de Oliveira, and C. Borges Margi are with the Department of Computer Engineering and Digital Systems, University of São Paulo, São Paulo 05508-900, Brazil (e-mail: renanalves@usp.br; lucasbg@usp.br; btrevizan@usp.br; cintia@usp.br).

F. Carvalho Lopes dos Santos is with the Department of Physiotheraphy, University of São Paulo, São Paulo 05508-900, Brazil (e-mail: fabiphisio@hotmail.com).

Color versions of one or more of the figures in this paper are available online at http://ieeexplore.ieee.org.

Digital Object Identifier 10.1109/JIOT.2015.2394493

the patient (in case, rehabilitation is done remotely). It should also allow sensors addition and (re)configuration in an intuitive fashion, so that a nontechnical user can run the system.

This paper is organized as follows. Section II discusses related work, and Section III describes the designed system, detailing the architecture and platforms used. Sections IV and V present communication and sensing design, implementation, results, and challenges faced while developing the system. Section VI concludes this paper and indicates future work.

II. Related Work

As mentioned earlier, significant effort has been taken to develop WSN-based eHealth systems [2], [3].

For instance, CodeBlue [6] is a project focused on offering a wireless communication infrastructure for several eHealth scenarios such as hospitals, patient first evaluation, and disaster emergencies. It also aims to be available at a number of platforms. Milosevic *et al.* [2] present another architecture proposal, focusing on ambulatory environment, yet not aiming to gather any specific data.

Motion tracking systems are a subclass of eHealth with its own peculiarities [4]. One approach is to use cameras to track human movements; however, it requires very specific setup, is highly costly, and does not use WSN.

In the realm of WSN, Mercury [7] is a framework that uses wearable devices to track and monitor motion activity for patients that suffer from neuromotor disorders.

Focusing on joint angle assessment, O'donovan *et al.* [8] describe an inertial and magnetic sensor-based technique for joint angle measurement, and later demonstrated it to measure knee and ankle joints angles [9]. Similar applications were proposed to assess upper limbs joint angle [10], [11].

Another motion tracking platform is Wagyromag [12], focused on data fusion and filtering. The authors claim that the platform may be of many uses, although only one of them was actually tested. Hipguard is a system to assess hip angle and load on each leg [13], and it is meant to monitor patients after surgery, aiding to avoid undesirable movements by emitting sound or a tactile warning. The system is also connected to a cellphone, which may be used to transmit data to a remote user, such as a physical therapist or a doctor.

In the context of hydrotherapy, joint angle assessment is not a simple task. Traditional measurement methods require visual feedback, which would require the physical therapist to submerge himself/herself in the pool to handle the instrument correctly. This procedure is not feasible, and a technological apparatus can provide a solution to the problem.

Silva *et al.* [14] proposed a hydrotherapy system based on a suit to monitor the backbone position and heart rate. The suit includes wired sensors to monitor the upper limb, that transmit sensed data to a floating wireless node, avoiding underwater communication. Next, the floating node transmits all the data received to a basestation through a wireless link. Although this application allows hydrotherapy monitoring, the mandatory use of a suit make it intrusive. To the best of our knowledge, it is the only previous effort in hydrotherapy monitoring.

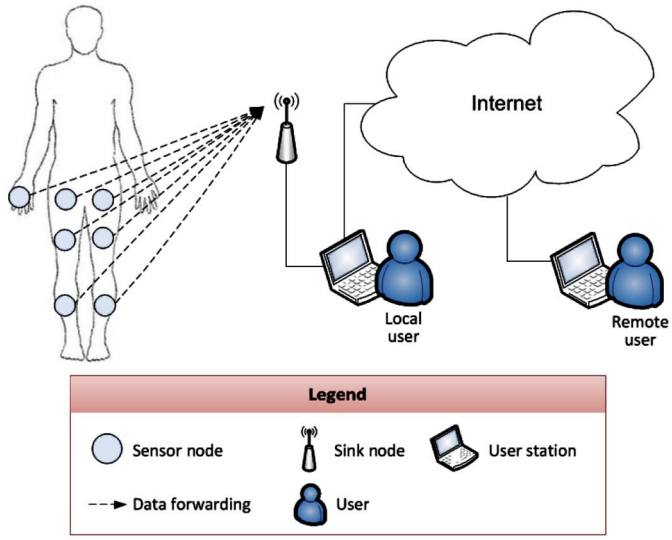

Fig. 1. System architecture.

Surveyed previous works do not present a comprehensive statistical analysis of the measurements obtained using described systems. Furthermore, comparing system response to traditional instruments, such as the goniometer, on actual patients has not been done, either. One of our accomplished goals is to demonstrate that the used class of inertial motion track systems is coherent with traditional measurement methods.

Furthermore, WSN-assisted hydrotherapy is nearly unexplored. We demonstrate that it is possible to conduct underwater radio communication in a long enough range to provide sensor nodes' data exchange to enable hydrotherapy.

III. System Description

This section describes the system designed to assist physical therapy concerning its objectives and architecture. Some hardware and software implementation possibilities are also discussed.

A. Objectives

The designed system aims to provide real-time supervision to physical therapy patients. This is done by assessing joint angles and other medical data, such as oxygen saturation and pulse, employing wireless sensing devices. The data collected should be available to a local user and to remote stations through the Internet as well.

B. Architecture

The system architecture is displayed in Fig. 1. Sensing nodes are attached to the patient body. Data is collected and sent to the local user computer through a basestation.

Data processing takes place at the local computer. The results are displayed to the user in real time and also stored for later use. Data should also be available to a remote user, such as a specialist doctor, connected through the Internet.

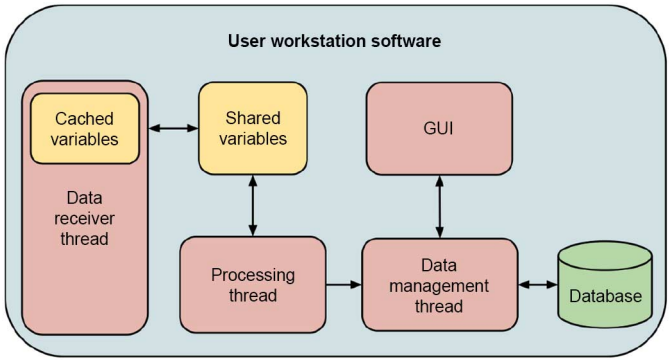

Fig. 2. Data processing software architecture.

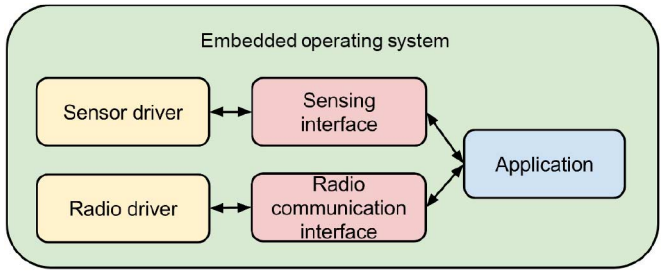

Fig. 3. Embedded software architecture.

C. Platforms

We tested a few implementation possibilities to the architecture presented. Sections III-C.1–C.3 describe the hardware and software employed in actual implementations.

1) Hardware: Several devices were used, each for a different purpose. To assess joint angle, we employed Shimmer version 2r motes [15], which have three-axis accelerometer and battery. An additional sensor may be coupled to the basic node, such as a magnetometer or electrocardiogram sensors. Along with Shimmer motes, a TelosB mote [16] is used as a basestation that interfaces with the computer.

An alternative implementation used the Microsoft .NET Gadgeteer platform. It is based on the FEZ Spider Mainboard [17], the main feature of which is its modularity. Sensors available in the toolkit include accelerometers, magnetometers, and pulse oximeter. Depending on the sensor attached to the mainboard, the node may assess joint angle and/or vital signs, or act as a basestation. Wireless communication is achieved through the IEEE 802.15.4 standard [18].

2) User Software: The software that runs in the user's computer and process sensor data is implemented according to the architecture depicted in Fig. 2.

This software is composed of two threads, besides the graphic interface threads. One of them, denominated "receiving thread," receives sensor data from the motes through the basestation. It also logs the data to a file.

The other thread, the "processing thread," processes all the data received from the other thread, according to the procedure described in the Appendix. The results are displayed at the graphical interface. This thread also records the maximum, minimum, and mean angle values at the end of the physical therapy session, stored for later analysis.

The database is modeled as three tables: 1) patient; 2) session; and 3) measurement. Information regarding patient personal data, physical therapist notes, and a measurement summary of each session are stored. The implementation used MySQL database manager.

To enhance user experience, a 3-D model of the patient is displayed to the user. The limbs are represented as cylinders and the hip as a triangle. Its position is determined by the nodes' sensed data.

3) Embedded Software: The software running on sensor nodes has three execution stages: 1) components initialization; 2) data sensing; and 3) data transmission. The architecture is depicted in Fig. 3.

The initialization stage sets up the accelerometer, communication module, and a timer, which triggers sensor readings. After initialization, while the system is used, a continuous periodic sequence of data sensing and transmission occurs.

One of the implementations was based on TinyOS [19] as underlying operating system, the main features of which are event-driven programming and design aimed at resource-constrained platforms. The program was coded with the nesC [20] programming language.

The other platform is .NET Gadgeteer, an open source toolkit by Microsoft. The programming language used is C# and the integrated development environment (IDE) was Microsoft Visual C# 2010 with .NET Micro Framework version 4.1.

IV. (Challenges to) Communication

This section aims to present and discuss the challenges faced throughout the prototype development regarding communication issues.

One of our prototypes was composed of six sensing nodes, whose data were directly transmitted to the basestation (single hop). The total payload size was 20 bytes, containing sensed data and application control fields. The default assessing rate was one measurement at each 128 ms.

All the data were sent through CSMA/CA mechanism from the IEEE 802.15.4 standard. Given the short distance between nodes in a star topology and the high data transmission rate, we noticed that packet loss occurred, and thus some measured angles were not smoothly plotted. In order to improve communication performance, we could increase frame interarrival, respecting application delay constrains; tweak the IEEE 802.15.4 parameters, such as backoff time and number of retries, since only fresh data are relevant; or use the contention free period available in the IEEE 802.15.4, which could limit the number of sensor nodes and the data transmission rate.

We made experiments in order to verify the possibility of adapting the system to hydrotherapy use. The major obstacle to accomplish this adaptation is to select the appropriate communication medium between the sensing nodes in underwater environment. Considering that underwater electromagnetic signal attenuation per inch is significantly higher if compared to the air, approaches to avoid radio communication should be a better fit.

Underwater acoustic communication is mainly used for long distances, as the confined space of a pool used in hydrotherapy would generate many interfering reflections. Also, the transceiver devices are usually too large to be used in a body area network (BAN).[1] Data transfer through light requires the transmitter and the receiver to be aligned, which is not the case in a BAN with mobile nodes [21].

Given the limitations presented by the first two alternatives we considered, we decided to actually measure how the radio-based communication would behave underwater. Experiments were conducted to plot the delivery rate versus distance curve. A connection should be established to send data through IEEE 802.15.4 devices. Early experiments revealed that the 2.4-GHz frequency is not appropriate to underwater environment, as the maximum range attained was around 20 cm. Due to that, lower frequency devices were sought. Most of the off-the-shelf devices are 2.4 GHz; acquiring a non-2.4-GHz IEEE 802.15.4 device and thus took about a year between finding and buying the device.

The transceiver was a 900-MHz XBee [22], deployed over an Arduino Uno [23], using an XBee shield. Transmitting data this way were not as simple as expected. Many parameters had to be configured through specific software from the manufacturer. In addition, there is no ready-to-use programming interface, and all the data must be raw treated through serial interface.

The experimental procedure consisted in positioning the devices at predefined distances and assessing the loss rate, to attain the point where communication loss would be too severe. The procedure took place in an actual hydrotherapy pool and made use of two devices, each one in a waterproof case, positioned such that the distance between the devices would be shorter than the distance between the devices and the surface or the floor. The sensed data are not affected by the fact that the sensing devices are underwater.

One of the devices sent data for 2 min and the other device only received and processed it. The data were actually a counter, used by the receiver to detect packet loss. The chart in Fig. 4 represents the received data percentage versus devices distance. Up to 75 cm, no losses at all are detected in the transmissions. From 80 cm onward, there are minor losses, reaching 96% delivering rate at 90 cm. However, from this point onward, communication gets unstable, reaching around 80% of receiving rate at 1m and zero at longer distances.

These data lead us to conclude that the system is portable to underwater environment, since 80 cm is enough to establish a communication link between sensing devices, with a 10-cm margin.

Be it land or underwater communication, both data should be secured to ensure health information privacy. In the BAN, data security can be provided by the use of the hardware security suite present in IEEE 802.15.4 [18] compliant devices, or by software implementation of security framework, such as TinySec [24] and ContikiSec [25]. For both cases, the prekeying approach should be adopted. For a secure communication over the Internet from a local workstation to the remote users, the recently released OpenSSL version (1.0.1g) [26] can be used.

[1]BAN is special purpose wearable WSN, limited to the human body area.

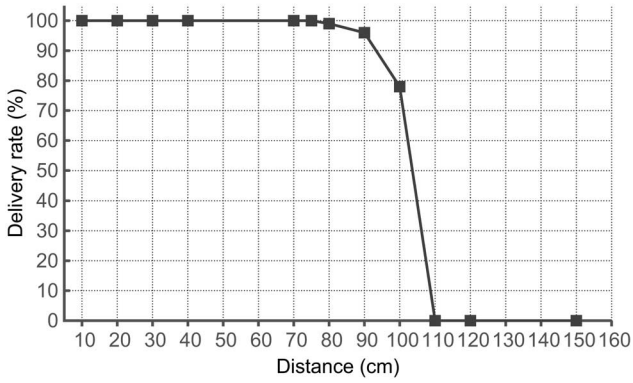

Fig. 4. Delivery rate versus node's distance in an underwater environment.

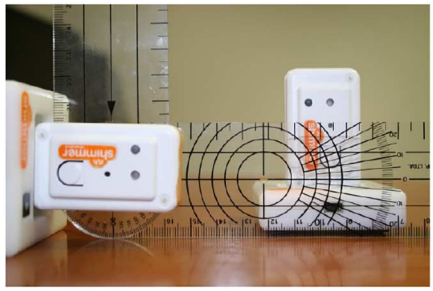

Fig. 5. Sensing nodes and goniometer positioning.

V. (Challenges in) Sensing

In this section, a discussion about acquiring sensor data is presented. The topics discussed include the sensing devices employed, prototype results, and caveats encountered.

A. Joint Angle Measurement

1) Sensor Details: The accelerometer available in Shimmer version 2r motes is the MMA7361L [27], which has reduced size, low current intake, and configurable sensitivity, set to the lowest value of $1.5g$, since large acceleration values are not expected and allow for better resolution.

2) Results: This section presents the angle measurement results. The first validation step is to confirm that the system measurements correspond to goniometer measurements.

The sensing nodes were attached to the goniometer, which was fixed to form the chosen angle. A total of four different angles were chosen from the interval [0°, 140°], which contains typical values of knee joint angle [5].

Two nodes were positioned parallel to each goniometer arm, so that both devices would measure the same angle. Fig. 5 illustrates this procedure.

Each reference angle was measured 20 times by the system. The reference angles were 0°, 45°, 90°, and 120°.

It is possible to establish the confidence interval (CI) for each measured angle with these data. The results are shown in Table I, for a confidence level of 95%.

The system mean error and its standard deviation are presented in Table II. Mean error was obtained by subtracting the measured angle from the reference angle. The standard

TABLE I
SYSTEM-MEASURED VALUES—STATISTICS

	Reference angle			
Statistics	0°	45°	90°	120°
Mean	1.70°	45.38°	90.43°	120.08°
CI length	0.45°	0.96°	0.83°	0.70°
Max error in CI	2.14°	1.34°	1.26°	0.77°

TABLE II
SYSTEM ERROR VALUES

Angle	Mean error	σ_{error}
0°	1.7°	1.4°
45°	0.4°	2.4°
90°	0.4°	2.1°
120°	0.1°	1.9°

Fig. 6. Sensing nodes and goniometer positioning on a patient.

deviation of the difference is composed of the system deviation and goniometer measurement error. The goniometer error was considered 1°, which is half of the smallest instrument precision.

The obtained errors are partially extrinsic to the system, as there are inherent goniometer measurement errors and misalignment between the nodes and instrument arms. Despite that, the mean error is small although its standard deviation is large. However, considering the 95% CI from Table I, the maximum error is not much larger than 2°.

The next validation step is to validate the system to joint angle measurement of human beings. The initial validation with an actual set up was conducted on the authors themselves.

Measurement experiments focused on the knee joint, according to the standard physical therapy procedure [5], with the patient in the supine position. To execute a joint flection, the hip must be 90°, avoiding rotation. Knee extension is obtained by returning from flection, on the sagittal plane.

The sensing nodes were positioned according to the goniometry procedure [5]. One of the devices was positioned parallel to lateral fibula, aligned to the lateral malleolus. The other mote was positioned parallel to the femur lateral surface, aligned to the larger trochanter. The distance from the nodes to the joint is long enough to avoid interference with the goniometer measurement. A positioning example is displayed in Fig. 6.

In preliminary tests, an enclosure made of cloth and hook-and-loop fastener was used to attach the nodes to the patients. However, this kind of enclosure causes large measurement errors, as the alignment is easily lost when the patient moves. Due to that, the nodes were attached by double-sided tape.

TABLE III
JOINT ANGLE MEASUREMENTS—FLECTION

Patient	Side	Goniometer mean	Standard deviation	System mean	Standard deviation
1	Right	132.5	2.2	137.9	1.8
1	Left	128.6	3.7	119.0	2.4
2	Right	136.2	2.3	139.9	0.9
2	Left	138.9	0.7	137.5	1.8
3	Right	132.2	1.3	128.9	3.1
3	Left	129.8	1.7	134.7	5.4

TABLE IV
JOINT ANGLE MEASUREMENTS—EXTENSION

Patient	Side	Goniometer mean	Standard deviation	System mean	Standard deviation
1	Right	12.9	2.6	11.0	1.2
1	Left	10.1	0.7	8.1	0.4
2	Right	8.0	2.4	4.6	1.9
2	Left	4.3	3.3	3.0	0.7
3	Right	3.6	2.6	6.8	1.1
3	Left	2.8	1.2	2.4	0.7

TABLE V
JOINT ANGLES—FLECTION

Patient	Side	Mean error	Error standard deviation	P	Reject H_0
1	Right	5.4	2.8	0.006	Yes
1	Left	9.6	2.9	0.006	Yes
2	Right	3.7	2.7	0.009	Yes
2	Left	1.4	1.8	0.056	No
3	Right	3.3	3.5	0.028	Yes
3	Left	4.9	4.5	0.021	Yes

TABLE VI
JOINT ANGLES—EXTENSION

Patient	Side	Mean error	Error standard deviation	P	Reject H_0
1	Right	1.9	3.1	0.074	No
1	Left	2.0	0.7	0.006	Yes
2	Right	3.4	2.1	0.008	Yes
2	Left	1.3	3.1	0.236	No
3	Right	3.2	2.0	0.008	Yes
3	Left	0.4	0.9	0.212	No

Ten measurements were made with the goniometer for each of the three patients, considering knee flection and extension. Simultaneously, system readings were captured.

Tables III and IV summarize the results following the procedure previously described. In most of the cases, goniometer measurements present larger standard deviation than our system, indicating that the system is more consistent in its measurements.

These data went through statistical analysis, and the results are presented in Tables V and VI. The mean error is calculated by the mean difference between paired measures. Absolute error values were larger if compared to the first experiment (static goniometer, without patients). This is expected due to misalignment between sensor nodes and the goniometer. The

TABLE VII
JOINT ANGLE—DATA GROUPING

Data grouping	*P*	Reject H_0
Patient 1 flection	0.167	No
Patient 2 flection	0.190	No
Patient 3 flection	0.632	No
Flection—all patients	0.911	No
Patient 1 extension	0.001	Yes
Patient 2 extension	0.004	Yes
Patient 3 extension	0.038	Yes
Extension—all patients	0.010	Yes
All measures	0.273	No

standard deviation value remained in the same magnitude, which supports the previous statement. Error values were inferior to 5° in most of the cases (10 out of 12), which is acceptable to physical therapy [28], [29].

The *P* values displayed in the tables are Wilcoxon Test [30] results, which is a nonparametric statistical test for paired data. The tested hypothesis (H_0) is that the difference between samples is null. The H_0 hypothesis is rejected if the *P* value is lower than significance level α, which is 0.05 considering 95% confidence level.

At this confidence level, H_0 is rejected in two-thirds of the cases, those holding larger mean errors. Two factors contribute to the adverse result in most of the cases. There is a small number of samples and the test used is sensitive to small samples [31]. In order to avoid this issue, measurement data were grouped; first left and right measurements, then patients data, and finally movements data. Results are displayed in Table VII. Only extension experiments presented adverse results. Regarding aggregate data, the test result is favorable to ensure system accuracy.

Previous works [2], [12] have applied more complex algorithms using data filters and other sensors, but have not shown that the results from their systems is similar to results from the goniometer.

Our initial validation for the joint angle measurements indicates that the system could effectively assist physical therapists.

B. Improving Joint Angle Measurement

This section presents the efforts to enhance joint angle measurement. One way to do that is by employing additional kinds of sensor to the nodes. Section V-A2 results were obtained by an accelerometer-only prototype version, which reduces system usage to assessing joint angles that vary only on one arbitrary vertical plane.

As described in the Appendix, an horizontal reference sensor would suffice to lift this limitation. A three-axis magnetometer was chosen for that matter; specifically, model HMC5843 [32], with maximum assessing rate at 100 Hz. It was assumed that the Earth's magnetic field is parallel to the ground and thus perpendicular to gravity.

It is essential to calibrate the sensor prior to use. The calibration procedure consists in finding the maximum and minimum values in each sensor axis, which should be equal to the Earth's magnetic field, in order to determine sensor offset. Data were collected by rotating the sensor in each of its axis on a flat surface. A total of 200 points were collected.

After calibration, we integrated the magnetometer to the prototype with accelerometers. As we tested this improved prototype, results were inadequate, being the magnetometer calibration the most probable error source.

Since the re-execution of calibration did not change the results, a reference magnetometer was used to assess the local magnetic field. It revealed that the magnetic field varied over time and according to the position. At a certain point, a value of $170,1\,\mu\mathrm{T}$ was measured, which is 7.5 times larger than the expected value of $23\,\mu\mathrm{T}$ of the Earth's magnetic field (estimation by the *The National Geophysical Data Center*). Furthermore, the magnetic field inclination is about 30° to the horizontal, which harms the results.

The calibration procedure was repeated, with a larger sample (6000 points) and at a location where the reference magnetometer indicated approximately constant magnetic field value ($2\,\mu\mathrm{T}$ at most). However, results were not different from the last calibration, differing by 1%.

A slightly different calibration procedure was attempted. The sensor was coupled to the reference magnetometer, willing to determine the maximum measured value at one of its axes, while the other axis was expected to be null. However, values indicated by sensor and reference magnetometer were not coherent. After testing, it was verified that the reference magnetometer interferes with sensor measures, which invalidates the calibration procedure.

A third calibration procedure was executed. It consisted in positioning the sensor at three arbitrary perpendicular positions, and in calculating the *offset* by solving an equation system. Nonetheless, results were not promising. A more elaborate calibration procedure is presented by Merayo *et al.* [33], although we did not test it due to its complexity, which would break our requirement of an easy-to-use system.

The joint angle measurement with accelerometer refers to the movement inherent acceleration. The procedure described in the Appendix assumes that the accelerometer senses only gravity acceleration. If assessing joint angle is desired while performing fast movements, it is necessary to filter accelerometer sensed values in order to distinguish gravity and movement acceleration, employing another sensor data if necessary.

C. Pulse Oximeter

In order to monitor medical data, we used a pulse oximeter module for the .NET Gadgeteer platform. The pulse oximeter module uses an LED to generate the wavelengths that are passed through the patient to a photodetector, providing the patient's O_2 saturation and pulse.

The programming methods provided by the .NET Gadgeteer framework return patient's pulse and blood oxygen rate. Sample results of the data collected are displayed in Table VIII. The column *Signal* represents the LED intensity control, which is responsible for increasing or decreasing the electric current, allowing a better reading from oxidation and pulse. The parameter *Signal* varies from 0 to 15.

TABLE VIII
PULSE OXIMETER MEASUREMENTS

Signal	Oxidation	Pulse
8	92	74
7	94	73
8	88	67
9	89	70
8	91	69
6	94	69
8	86	72

VI. CONCLUSION

WSNs and IoT have been used to build several eHealth systems. Our focus is assisting physical therapy, which is a particular case of such systems, with specific characteristics and requirements, concerning equipment, software, and system.

We presented a system architecture designed to assist physical therapy. The system objectives are to assess patient's joint angles and vital signs. The architecture is open and generic enough to be implemented in several platforms, as demonstrated with two prototypes implemented in TinyOS/Shimmer and .NET Gadgeteer.

In addition to the flexible architecture, our results demonstrate that inertial join angle measurement systems are compliant with a traditional physical therapy instrument, the goniometer. This conclusion is supported by measurement experiments comparing results from human subjects.

Another novel result concerns adapting the system to hydrotherapy. There is a lack of tools to assist this kind of therapy. The experiments show that it is possible to assess joint angles in a hydrotherapy pool employing off-the-shelf 900-MHz communication radios.

Future work includes conducting experiments for a wider range of joints, testing QoS over the Internet, and adapting the systems from star to multihop topology. We would also like to make a larger scale evaluation of human subjects.

APPENDIX
ANGLE CALCULATION PROCEDURE

An angle θ formed by two vectors $\boldsymbol{v}_1$ and $\boldsymbol{v}_2$ may be calculated from the vectors coordinates in an Euclidean space with the arc-cosine expression $\left(\theta = \arccos\left(\frac{\boldsymbol{v}_1 \cdot \boldsymbol{v}_2}{|\boldsymbol{v}_1||\boldsymbol{v}_2|}\right)\right)$, considering an orthonormal base.

In order to determine patient's joint angles, it is enough to obtain vectors in the same directions as the angle measurement lines. It is crucial that both vectors are on a common base. These vectors may be obtained by sensor motes coupled to the patient.

To allow the sensor mote direction in space, the following premises are made.

1) The environment base $B = (b_x, b_y, b_z)$, common to all sensing nodes, is fixed. We convene that $\boldsymbol{b}_z$ is a unit vector parallel to gravity, $\boldsymbol{b}_x$ is a horizontal unit vector, perpendicular to $\boldsymbol{b}_z$, and $\boldsymbol{b}_y$ is equal to the vector product of the other two vectors.
2) Each sensor node has an intrinsic base. It varies concerning the environment base. All the sensor node measurements are made with respect to this base.
3) sensor nodes are capable of assessing components $\boldsymbol{b}_z$ and $\boldsymbol{b}_x$ of the environment base on its intrinsic base.
4) One of the sensor node axes should be aligned to the anatomical point observed. We convene that it is the *x*-axis.

Thus, the problem of calculating the sensor node direction in space is reduced to calculating the *x*-axis direction in terms of the environment base.

Let $\boldsymbol{u} = (u_x, u_y, u_z)$ and $\boldsymbol{v} = (v_x, v_y, v_z)$ be the normalized vectors representing the measured values of b_x e b_z. Therefore, $\boldsymbol{v}$ represents the gravity direction and $\boldsymbol{u}$ represents the horizontal reference vector, both represented by the means of the node intrinsic base.

The change-of-basis matrix M_{ne} is the matrix that, if multiplied from the right by a vector, transforms its coordinates on the environment base into coordinates on the intrinsic base of the node. The environment horizontal reference is related to vector $\boldsymbol{u}$ by the following equation: $M_{\mathrm{ne}}.(1,0,0) = (u_x, u_y, u_z)$. Similarly, the equation $M_{\mathrm{ne}}.(0,0,1) = (v_x, v_y, v_z)$ relates the gravity-oriented unit vector to the valued measured by the sensor node. Finally, the vector products are related by $M_{\mathrm{ne}}.(0,1,0) = \boldsymbol{u} \times \boldsymbol{v}$.

With this information, it is possible to write M_{ne}, as stated in (1). Once M_{ne} is available, the vector that indicates the *x*-axis direction is attainable by the following equation: $M_{\mathrm{ne}}.(x,y,z) = (1,0,0)$

$$M_{\mathrm{ne}} = \begin{bmatrix} u_x & v_y.u_z - v_z.u_y & v_x \\ u_y & v_z.u_x - v_x.u_z & v_y \\ u_z & v_x.u_y - v_y.u_x & v_z \end{bmatrix}. \quad (1)$$

The values of x, y, and z obtained by resolving the system of equations are the coordinates of the sensor node *x*-axis unit vector, in environment base terms. To calculate the angle between two sensor nodes, it is enough to obtain both nodes' *x*-axis direction and input it at the arc-cosine equation.

For the purposes of the prototype, an accelerometer is used to evaluate b_z. Each sensor offset was calibrated following the recommended procedure [34]. No sensor was employed to obtain a horizontal reference, which was fixed to a constant value. Due to this simplification, the system will work properly only if both sensor nodes are in a common vertical plan. This restriction may be lifted by adding an appropriate sensor, such as a magnetometer or gyroscope.

ACKNOWLEDGMENT

The authors would like to thank the Laboratory of Computer Networks and Architecture (LARC/USP) for providing the necessary infrastructure.

REFERENCES

[1] L. Atzori, A. Iera, and G. Morabito, "The Internet of Things: A survey," *Comput. Netw.*, vol. 54, no. 15, pp. 2787–2805, 2010.
[2] A. Milenkovic, C. Otto, and E. Jovanov, "Wireless sensor networks for personal health monitoring: Issues and an implementation," *Comput. Commun.*, vol. 29, pp. 2521–2533, 2006.
[3] H. Alemdar and C. Ersoy, "Wireless sensor networks for healthcare: A survey," *Comput. Netw.*, vol. 54, no. 15, pp. 2688–2710, 2010.

[4] A. Hadjidj, M. Souil, A. Bouabdallah, Y. Challal, and H. Owen, "Review: Wireless sensor networks for rehabilitation applications: Challenges and opportunities," *J. Netw. Comput. Appl.*, vol. 36, no. 1, pp. 1–15, Jan. 2013.
[5] L. Palmer, M. Epler, and M. Epler, *Fundamentals of Musculoskeletal Assessment Techniques*. Philadelphia, PA, USA: Lippincott, 1998.
[6] D. Malan, T. Fulford-jones, M. Welsh, and S. Moulton, "Codeblue: An *ad hoc* sensor network infrastructure for emergency medical care," in *Proc. Int. Workshop Wearable Implantable Body Sensor Netw.*, 2004.
[7] K. Lorincz *et al.*, "Mercury: A wearable sensor network platform for high-fidelity motion analysis," in *Proc. 7th ACM Conf. Embedded Netw. Sensor Syst (SenSys'09),* 2009, pp. 183–196.
[8] K. O'Donovan, R. Kamnik, D. O'Keeffe, and G. Lyons, "An inertial and magnetic sensor based technique for joint angle measurement," *J. Biomech.*, vol. 40, no. 12, pp. 2604–2611, 2007.
[9] K. O'Donovan and S. Ayer, "Real-time joint angle measurement using the shimmer wireless sensor platform," in *Proc. 1st ACM Workshop Mob. Syst., Appl., Serv. Healthcare (mHealthSys'11)*, 2011, pp. 7:1–7:2.
[10] Y. Jung, D. Kang, and J. Kim, "Upper body motion tracking with inertial sensors," in *Proc. IEEE Int. Conf. Robot. Biomimet. (ROBIO'10)*, Dec. 2010, pp. 1746–1751.
[11] A. Hadjidj, A. Bouabdallah, and Y. Challal, "Rehabilitation supervision using wireless sensor networks," in *Proc. IEEE Int. Symp. World Wireless, Mob. Multimedia Netw. (WoWMoM'11)*, Jun. 2011, pp. 1–3.
[12] A. Olivares, G. Olivares, F. Mula, J. Gorriz, and J. Ramirez, "Wagyromag: Wireless sensor network for monitoring and processing human body movement in healthcare applications," *J. Syst. Archit.*, vol. 57, no. 10, pp. 905–915, 2011.
[13] P. Iso-Ketola, T. Karinsalo, and J. Vanhala, "Hipguard: A wearable measurement system for patients recovering from a hip operation," in *Proc. 2nd Int. Conf. Pervasive Comput. Technol. Healthcare (PervasiveHealth'08)*, Jan. 2008, pp. 196–199.
[14] H. Silva *et al.*, "Wireless hydrotherapy smart-suit network for posture monitoring," in *Proc. IEEE Int. Symp. Ind. Electron. (ISIE'07)*, Jun. 2007, pp. 2713–2717.
[15] Shimmer Res., *Shimmer2r—Wireless Sensor Platform*, Boston, MA, USA, 2011.
[16] MEMSIC Inc., Andover, MA, USA (2004). "telosB product details—6020-0094-04 Rev B.," [Online]. Available: http://www.memsic.com
[17] G. Electronics. (2012). *Fez Spider Mainboard* [Online]. Available: http://www.ghielectronics.com/catalog/product/269
[18] *IEEE Standard for Local and Metropolitan Area Networks—Part 15.4: Low-Rate Wireless Personal Area Networks (LR-WPANs)*, IEEE Standard 802.15.4-2011, 2011.
[19] P. Levis *et al.*, "TinyOS: An operating system for sensor networks ambient intelligence," in *Ambient Intelligence*, W. Weber, J. M. Rabaey, and E. Aarts, Eds. Berlin, Germany: Springer-Verlag, 2005, ch. 7, pp. 115–148.
[20] D. Gay *et al.*, "The NESC language: A holistic approach to networked embedded systems," in *Proc. Program. Language Design Implement. (PLDI)*, 2003, pp. 1–11.
[21] X. Che, I. Wells, G. Dickers, P. Kear, and X. Gong, "Re-evaluation of RF electromagnetic communication in underwater sensor networks," *IEEE Commun. Mag.*, vol. 48, no. 12, pp. 143–151, Dec. 2010.
[22] Digi Int. (2014). "XBee module," Minnetonka, MN, USA [Online]. Available: http://www.digi.com/pdf/ds_xbeemultipointmodules.pdf
[23] Arduino. (2014) "Arduino Uno," [Online]. Available: http://arduino.cc/en/Main/arduinoBoardUno
[24] C. Karlof, N. Sastry, and D. Wagner, "Tinysec: A link layer security architecture for wireless sensor networks," in *Proc 2nd Int. Conf Embedded Netw. Sens. Syst.*, 2004, pp. 162–175.
[25] L. Casado and P. Tsigas, "ContikiSec: A secure network layer for wireless sensor networks under the Contiki operating system," in *NordSec*, vol. 5838. New York, NY, USA: Springer, 2009, pp. 133–147.
[26] OpenSSL Project. *OpenSSL cryptography and SSL/TLS toolkit* [Online]. Available: http://www.openssl.org/, accessed Mar. 2014.
[27] Freescale Semiconductor Inc., Austin, TX, USA (2008). "±1.5g, ±6g three axis low-g micromachined accelerometer," MMA7361L Data Sheet [Online]. Available: http://www.pololu.com/file/0J379/MMA7341L.pdf
[28] K. W. Hayes, "The effect of awareness of measurement error on physical therapists' confidence in their decisions," *Phys. Therapy*, vol. 72, no. 7, pp. 515–525, 1992.
[29] G. R. F. Bertolini *et al.*, "Avaliao dos métodos de alongamento estãtico e alongamento estãtico combinado ao ultra-som na extensibilidade do gastrocnłmico," *Fisioter. mov.*, vol. 1, no. 21, pp. 115–122, 2008.
[30] F. Wilcoxon, "Individual comparisons by ranking methods," *Biometr. Bull.*, vol. 1, no. 6, pp. 80–83, 1945.
[31] N. Feltovich, "Nonparametric tests of differences in medians: Comparison of the Wilcoxonmann-Whitney and robust rank-order tests," *Exp. Econom.*, pp. 6–273, 2003.
[32] Honeywell Int. Inc., Morristown, NJ, USA (2009). "3-Axis digital compass IC HMC5843," HMC5843 Data Sheet [Online]. Available: http://www51.honeywell.com/aero/common/documents/myaerospacecatalog-documents/Defense_Brochures-documents/HMC5843.pdf
[33] J. M. G. Merayo, P. Brauer, F. Primdahl, J. R. Petersen, and O. V. Nielsen, "Scalar calibration of vector magnetometers," *Meas. Sci. Technol.*, vol. 11, pp. 120–132, 2000.
[34] *9DOF Calibration User Manual*, Rev 1.0b, Shimmer Res., Boston, MA, USA, 2012, 107 pp.

Renan C. A. Alves was born in São Bernardo do Campo, São Paulo, Brazil, in 1989. He received the B.S. degree in electrical engineering and M.Sc. degree from the University of São Paulo, São Paulo, Brazil, in 2011 and 2014, respectively.

His research interests include network protocol modeling and performance analysis, and wireless sensor networks protocols and applications.

Lucas Batista Gabriel was born in Mogi das Cruzes, São Paulo, Brazil, in 1992. He is currently working toward the degree in computer engineering at Escola Politécnica (Poli-USP), University of São Paulo, São Paulo, Brazil.

His research interests include software-defined wireless networks and mobile sensing devices.

Bruno Trevizan de Oliveira was born in Santos, São Paulo, Brazil, in 1984. He received the B.S. degree in information systems and Master's degree in computing engineering from the University of São Paulo, São Paulo, Brazil, in 2009 and 2012, respectively, and is currently working toward the Ph.D. degree in computing engineering at Escola Politécnica (Poli-USP), University of São Paulo, São Paulo, Brazil.

His research interests include applied cryptography, security in wireless sensor networks, and software-defined wireless networks.

Cíntia Borges Margi (M'03) received the B.S. degree in electrical engineering and M.Sc. degree from the University of São Paulo, São Paulo, Brazil, in 1997 and 2000, respectively, and the Ph.D. degree in computer engineering from the University of California Santa Cruz, Santa Cruz, CA, USA, in 2006.

She has been an Assistant Professor with the University of São Paulo, since 2007. Since 2010, she has been associated with the Department of Computer Engineering and Digital Systems (PCS/EPUSP), and from 2007 to 2010, she was involved with the Information Systems course at EACH/USP. Her research interests include wireless sensor networks (protocols, systems, security, energy consumption, and management) and software-defined wireless networks.

Fabíola Carvalho Lopes dos Santos was born in São Paulo, Brazil, in 1974. She received the B.S. degree in physiotherapy and Master's degree in rehabilitation sciences from the University of São Paulo, São Paulo, Brazil, in 1999 and 2012, respectively, and is currently working toward the Ph.D. degree in rehabilitation sciences at the University of São Paulo.

Her research interests include applied posture assessment and aquatic therapy (hydrotherapy).